PERGAMON

Carbon 41 (2003) 1801–1807

CARBON

Complex permittivities and dielectric relaxation of granular activated carbons at microwave frequencies between 0.2 and 26 GHz

James E. Atwater*, Richard R. Wheeler Jr.

UMPQUA Research Company, P.O. Box 609, Myrtle Creek, OR 97457 USA

Received 5 October 2001; accepted 26 March 2003

Abstract

Carbonaceous materials are amenable to microwave heating to varying degrees. The primary indicator of susceptibility is the complex permittivity (ϵ^*), of which the real component correlates with polarization and the imaginary term represents dielectric loss. For a given material, the complex permittivity is dependent upon both frequency and temperature. Here we report the complex permittivities of three activated carbons of diverse origin over the frequency range from 0.2 to 26 GHz. Dielectric polarization–relaxation phenomena for these materials are also characterized. Measurements were made using a coaxial dielectric probe and vector network analyzer based system across the temperature region between 22 and 190 °C.

Keywords: A. Activated carbon; D. Dielectric properties

1. Introduction

Many granular activated carbons are highly susceptible to microwave (dielectric) heating. This may be used to advantage in the thermal treatment of activated carbons and in the thermal regeneration of loaded activated carbon based sorbents via high frequency irradiation [1]. However, much variability is evident between different forms of activated carbon. To provide a quantitative view of the extent of this variability, complex permittivities of three activated carbons were determined at microwave frequencies between 0.2 and 26 GHz, and over the approximate temperature range 22–190 °C.

Dielectric heating through absorption of radiation at microwave frequencies involves phenomena such as induced electronic, atomic, and space charge polarizations, or the direct coupling of electromagnetic radiation with rotational and vibrational transitions of susceptible dielectric materials to produce heat. As with other regions of the electromagnetic spectrum, microwave transmission and reflections are governed by Maxwell's equations

$$\nabla \times \boldsymbol{E} = i\omega\mu^*\boldsymbol{H} \tag{1}$$

$$\nabla \cdot (\varepsilon^*\boldsymbol{E}) = 0 \tag{2}$$

$$\nabla \times \boldsymbol{H} = -i\omega\varepsilon^*\boldsymbol{E} \tag{3}$$

$$\nabla \cdot \boldsymbol{H} = 0 \tag{4}$$

where $\boldsymbol{E}$ and $\boldsymbol{H}$ are the time-varying electric and magnetic field vectors, and μ^* and ϵ^* are the permeability and permittivity of the medium, respectively [2]. In nonmagnetic media, susceptibility to microwave heating is governed by the frequency (ω) dependent complex permittivity [3,4]

$$\epsilon^*(\omega) = \epsilon'(\omega) - i\epsilon''(\omega) \tag{5}$$

The ϵ^* terms are described by the Kramers–Kronig relations

$$\varepsilon'(\omega) = \varepsilon_\infty + \frac{2}{\pi}\int_0^\infty \frac{\varepsilon''(\omega)\omega'}{(\omega')^2 - \omega^2}\,\mathrm{d}\omega' \tag{6}$$

$$\varepsilon''(\omega) = \frac{2}{\pi}\int_0^\infty \frac{[\varepsilon'(\omega) - \varepsilon_\infty]\,\omega}{(\omega')^2 - \omega^2}\,\mathrm{d}\omega' \tag{7}$$

where ϵ_∞ is permittivity at the high frequency limit, and ω'

*Corresponding author. Fax: +1-541-863-7775.
E-mail address: jatwater@urcmail.net (J.E. Atwater).

0008-6223/03/$ – see front matter
doi:10.1016/S0008-6223(03)00150-7

is an integration variable [5]. In the complex plane, the real and imaginary terms of $\epsilon^*(\omega)$ correlate with polarization and energy loss, respectively. The dielectric loss factor or dissipation factor ($\tan\delta$) is defined as

$$\tan\delta = \frac{\omega\varepsilon''(\omega)\,|\boldsymbol{E}_o|^2}{\omega\varepsilon'(\omega)|\boldsymbol{E}_o|^2} = \frac{\varepsilon''(\omega)}{\varepsilon'(\omega)} \tag{8}$$

This represents the fractional power loss as compared to power stored. The average power per unit volume (P) consumed by loss mechanisms can then be calculated as

$$P = 1/2\omega\varepsilon''|\boldsymbol{E}_o|^2 \tag{9}$$

The attenuation of a microwave beam directed along the x axis by an absorbing material is described by [6]

$$P(x) = P_o \exp(-2\alpha x) \tag{10}$$

where the attenuation coefficient (α) is a function of the angular frequency (ω), complex permittivity, and complex permeability (μ^*)

$$\alpha = \omega\sqrt{\sqrt{\varepsilon'^2+\varepsilon''^2}\sqrt{\mu'^2+\mu''^2}} \times \sin\left[\frac{\arctan\left(\frac{\varepsilon''}{\varepsilon'}\right)+\arctan\left(\frac{\mu''}{\mu'}\right)}{2}\right] \tag{11}$$

In nonmagnetic materials, values of μ^* are extremely low, hence, microwave absorption is dominated by the complex permittivity terms. From this, it is clear that knowledge of the frequency and temperature dependencies of complex permittivity in the microwave region of the electromagnetic spectrum for a given granular activated carbon may be quite useful in the modeling and design of dielectric heating systems.

2. Experimental

The complex permittivity measurement apparatus is illustrated schematically in Fig. 1. The integrated system consists of the following components: HP8722D vector network analyzer (VNA), HP85070B coaxial dielectric probe, HP85056A calibration kit, and HP85130F adapter kit. While the HP8722D VNA was capable of operation between 0.05 and 40 GHz, limitations of the dielectric probe and associated transmission elements reduced the practical working frequency range to 0.2–26 GHz. Also, dissipation ($\tan\delta$) factors $\geqslant$0.05 are required to assure accuracy of the test results. Complex permittivity measurements were made under software control via a Hewlett-Packard interface bus (HPIB) parallel connection between the computer and the VNA. In operation, the VNA scans a preset frequency range over which transmission and reflection parameters are determined. Material in direct contact with the coaxial dielectric probe alters the phases and magnitudes of reflected power observed by the VNA. Complex permittivities were calculated from the measured transmission and reflection parameters using HP85071B software. Experiments conducted to confirm the validity of data obtained using this system have been described previously [7,8].

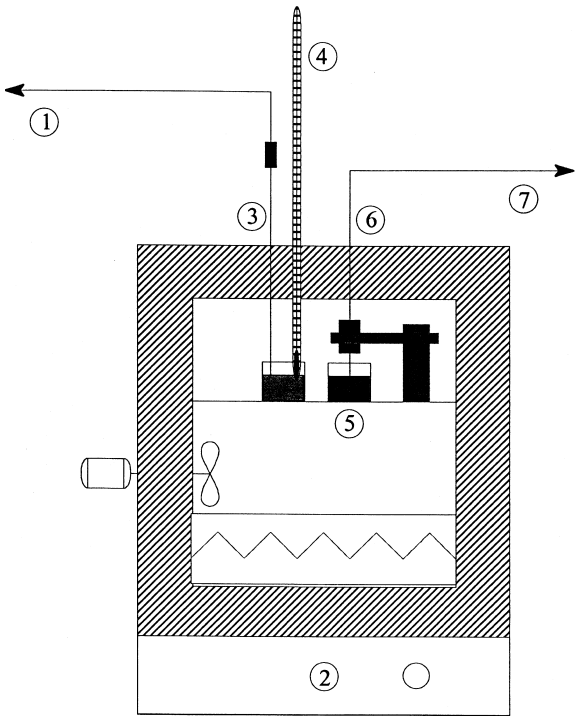

Fig. 1. Complex permittivity test apparatus: (1) temperature controller, (2) oven, (3) thermocouple, (4) Hg thermometer, (5) coaxial dielectric probe immersed in sample, (6) high-temperature semi-rigid coaxial cable, (7) vector network analyzer, and computer.

To measure complex permittivities at elevated temperatures, the coaxial dielectric probe was mounted inside a gravity convection oven. To minimize temperature gradients, the oven was modified by sealing the external air convection current ports, and by the addition of an internal recirculation fan. Improved temperature control was achieved using a digital PID controller and a K-type thermocouple probe mounted inside the oven. A 610-mm precision mercury thermometer covering the temperature range between -1 and 201 °C with 0.2 °C resolution was used to monitor the temperature of the test specimen. Both the thermocouple probe and the mercury thermometer were inserted into a sand-filled beaker of equivalent volume and elevation within the oven as the material under study. A high temperature semi-rigid coaxial cable was used to connect the oven mounted dielectric probe with the external VNA. Access for the thermocouple, thermometer, and coaxial cable was established through a 5.0-cm

diameter insulation filled circular opening at the top of the oven. Temperature regulation was accurate to within 0.2 °C.

The complex permittivities of three activated carbons were determined at five temperatures covering the range 22–190 °C. Samples were presented to the instrument as fine powders, thus obviating the need to correct for the effects of intergranular porosity [9–13]. To minimize interference from adsorbed water, each activated carbon was dried at 180 °C for a minimum of 72 h, and then stored in a desiccator prior to analysis. The instrument was first calibrated, followed by duplicate measurements at ambient temperature, with the dielectric probe in intimate contact with the material under study. The temperature was then increased. Once the set-point temperature was reached, a period of 45 min was allowed for the system to stabilize. Then a second set of duplicate measurements were made. This procedure was followed until data covering the full temperature span were gathered. The numerical values of all complex permittivities were calculated as dimensionless relative permittivities (ϵ^*/ϵ_o). These may be converted to absolute permittivities through multiplication by the permittivity of free space (ϵ_o), in appropriate units.

3. Results and discussion

Temperature dependent complex permittivities were determined and dielectric polarization–relaxation phenomena were characterized for commercially available granular activated carbons prepared from coal, peat, and coconut shell. The experimental results indicate a significant degree of variation between these different activated carbon types. The real and imaginary components of the complex permittivities for these three materials as functions of both frequency and temperature are presented in Figs. 2–4, respectively.

3.1. Calgon APA

Calgon APA is an acid washed activated carbon prepared from low ash and low sulfur bituminous coals and activated thermally in a rotary kiln. The material is widely used in a variety of industrial separation and purification applications. Researchers in our laboratory have employed it as an adsorbent in the design of several water purification systems for regenerative life support applications aboard manned spacecraft [14].

The complex permittivities shown in Fig. 2 indicate that this activated carbon interacts quite strongly over this frequency range. At each temperature, the real component of the complex permittivity decreases smoothly with increasing frequency. Maxima are evident at the low frequency limit (0.2 GHz), with ϵ' values increasing with temperature from 78 at 24 °C to 110 at 189 °C. At

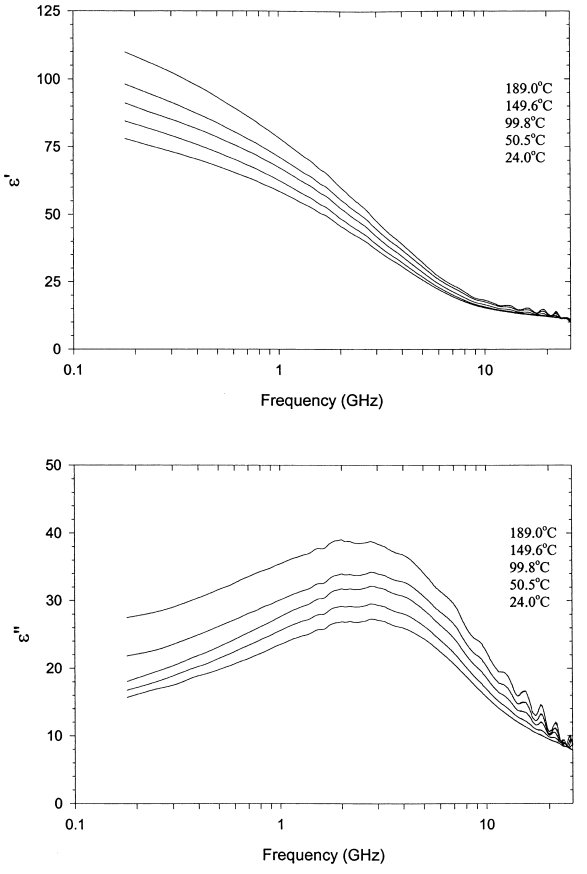

Fig. 2. Complex permittivities of Calgon APA bituminous activated carbon.

frequencies above 23 GHz, ϵ' values for all temperatures converge, yielding minimum values of ~11 at the high frequency limit (26 GHz). Dielectric loss factors (ϵ'') increase with frequency to maximum values near 2.8 GHz and then decrease to minimum values at the high frequency limit. Dielectric loss is temperature dependent across the full spectrum, strongly between 0.2 and 10 GHz, and progressively less so at higher frequencies. Dielectric loss maxima range from 27.3 at 24 °C to 39.0 at 189 °C. Dissipation factors vary between 0.649 and 0.726 over this temperature range.

3.2. Alltech 5769

This material consists of analytical laboratory grade coconut shell activated carbon. It is most commonly used in sampling and concentration of volatile organic vapors, such as in purge and trap gas chromatography. It interacts considerably less strongly across the full microwave spectrum than for the previous example (Fig. 3). For each temperature, the real component of the complex permittivity decreases smoothly with increasing frequency. Maxi-

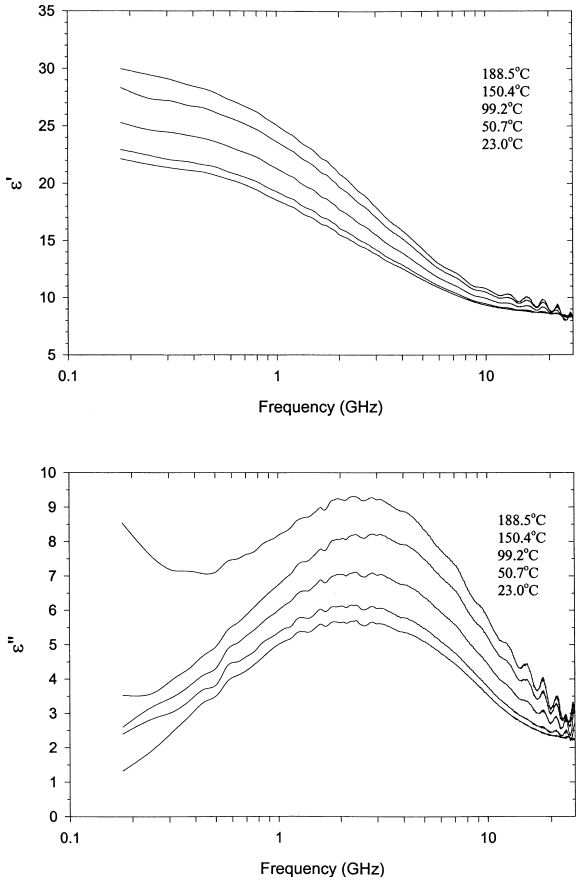

Fig. 3. Complex permittivities of Alltech 5769 coconut shell activated carbon.

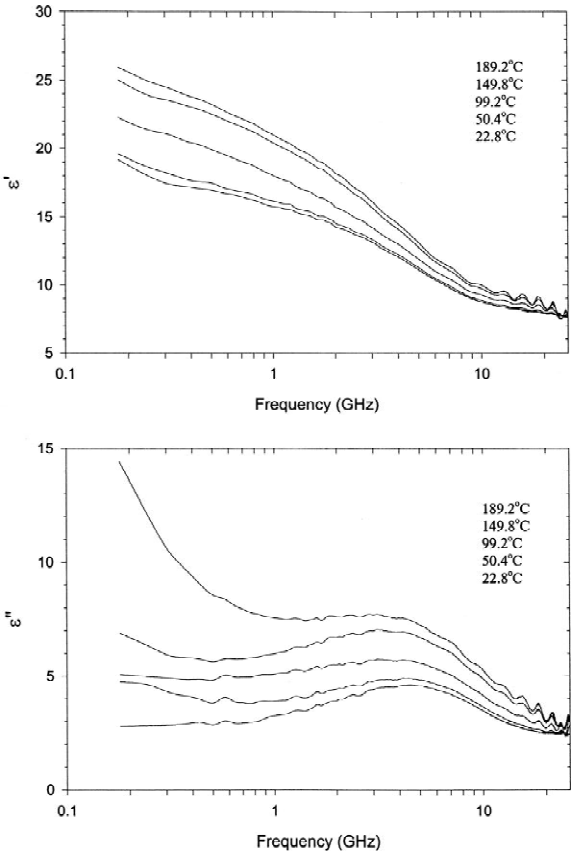

Fig. 4. Complex permittivities of Sigma C-3014 kilned peat activated carbon.

mum ϵ' values occur at the low frequency limit (0.2 GHz) which increase with temperature from 22.1 at 23 °C to 30.0 at 188.5 °C. The magnitude of this temperature dependence diminishes with increasing frequency. Between 23 and 150.4 °C, dielectric losses generally increase with frequency to maximum values in the range 2.3–2.8 GHz. However, at the highest temperature, a secondary maximum of 8.5 occurs at the low frequency limit. For this activated carbon specimen, the magnitude of ϵ'' is temperature dependent across the full spectrum. Maxima range from 5.7 at 24 °C to 9.3 at 191 °C, corresponding to tan δ values which increase smoothly from 0.386 to 0.442 over this temperature span. Between 150.4 and 188.5 °C, the strongest temperature effects on ϵ'' are evident at frequencies below 0.5 GHz. For lower temperatures, the strongest effects are seen between 2 and 5 GHz.

3.3. Sigma C-3014

This relatively impure activated carbon with a specific surface area of ~600 m^2/g is prepared by kiln firing of carbonaceous materials obtained from peat bogs. It is employed as a general adsorbent in the laboratory, as, for example, in the removal of impurities during organic synthesis.

The complex permittivity data illustrated in Fig. 4 indicate a slightly weaker interaction with microwaves over this frequency range than for the previous specimen. As with the other carbons tested, ϵ' decreases smoothly with increasing frequency. Maximum ϵ' values occur at the low frequency limit. These increase with temperature from 19.2 at 22.8 °C to 25.9 at 189.2 °C. The magnitude of temperature dependence generally diminishes with increasing frequency. The point of maximum dielectric loss progressively shifts toward lower frequencies as temperature increases. Values range from 4.6 at 4.53 GHz and 22.8 °C to 7.7 at 2.84 GHz and 189.2 °C. For all measurements made above ambient temperature, secondary maxima are evident at 0.2 GHz. Temperature dependence of ϵ'' is observed across the full spectrum. Dissipation factors increase smoothly with temperature from 0.399 at 22.8 °C to 0.469 at 189.2 °C.

3.4. Polarization–relaxation phenomena

In susceptible solids, heat is produced via oscillating induced interfacial (Maxwell–Wagner) and space-charge polarizations. Polarization–relaxation phenomena have been described by Debye [15] as

$$\varepsilon^*(\omega) = \varepsilon_\infty + \frac{\varepsilon_s - \varepsilon_\infty}{1 + i\omega\tau} \tag{12}$$

where ϵ_s is the static (zero frequency) permittivity, ε_∞ is the permittivity at the high frequency limit, and τ represents the polarization relaxation time, which is the inverse of the frequency of maximum dielectric loss [16–22]. The real and imaginary components of the complex permittivity are then described as

$$\varepsilon'(\omega) = \varepsilon_\infty + \frac{\varepsilon_s - \varepsilon_\infty}{1 + (\omega\tau)^2} \tag{13}$$

$$\varepsilon''(\omega) = \frac{\varepsilon_s - \varepsilon_\infty}{1 + (\omega\tau)^2} \cdot \omega\tau \tag{14}$$

In the slightly more complex Cole–Cole model [16,17] the $i\omega\tau$ term is raised to the power of β, where $\beta \leq 1$. Here, the polarization and dielectric loss terms can be described as [18]

$$\varepsilon'(\omega) = \varepsilon_\infty + \frac{(\varepsilon_s - \varepsilon_\infty)}{2} \cdot \left[1 - \frac{\sinh(\beta \ln \omega\tau)}{\cosh(\beta \ln \omega\tau) + \cos\left(\frac{\beta\pi}{2}\right)} \right] \tag{15}$$

$$\varepsilon''(\omega) = \frac{(\varepsilon_s - \varepsilon_\infty)\sin\left(\frac{\beta\pi}{2}\right)}{2\left[\cosh(\beta \ln \omega\tau) + \cos\left(\frac{\beta\pi}{2}\right)\right]} \tag{16}$$

From these relations, it follows that a plot of ϵ'' versus ϵ' in the complex plane, termed a Cole–Cole plot, will form a semi-circle centered at

$$\varepsilon'(\omega) = \frac{\varepsilon_s + \varepsilon_\infty}{2} \tag{17}$$

in which β is the central angle of circular arc for the dielectric loss.

Cole–Cole plots for the three carbons included in this study are presented in Figs. 5–7. The various symbols depict experimental data acquired at the indicated temperatures. The lines drawn through the symbols represent the values calculated using Eqs. (15) and (16) from the parameters summarized in Table 1. As shown in Fig. 5, the experimental data from the coconut shell activated carbon (Alltech 5769) are in reasonably good agreement with the calculated values, with minor deviations evident at the high frequency limit (left hand side of the Cole–Cole plot). Minor deviations also occur near the low frequency end of the spectrum (right hand side of Cole–Cole plot) for the highest temperature point (188.5 °C). This is most

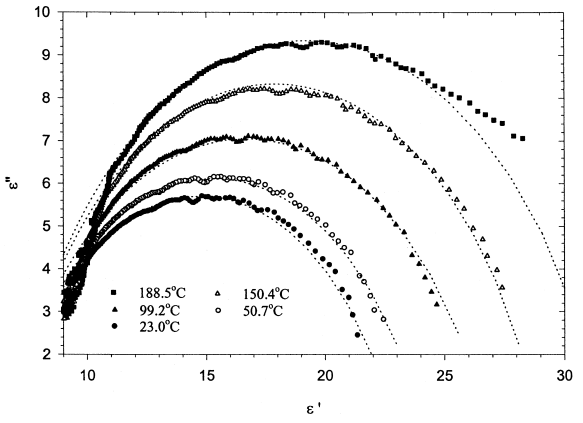

Fig. 5. Cole–Cole plot for Alltech 5769 coconut shell activated carbon.

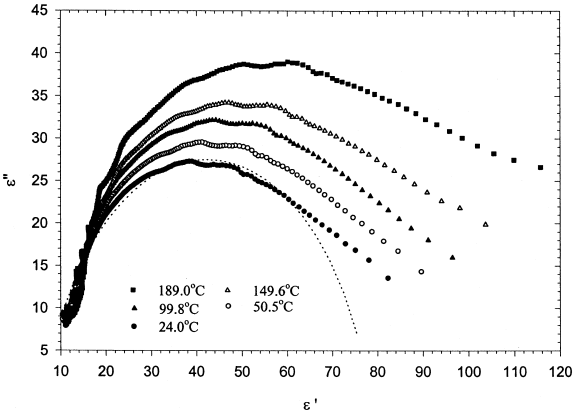

Fig. 6. Cole–Cole plot for Calgon APA bituminous activated carbon.

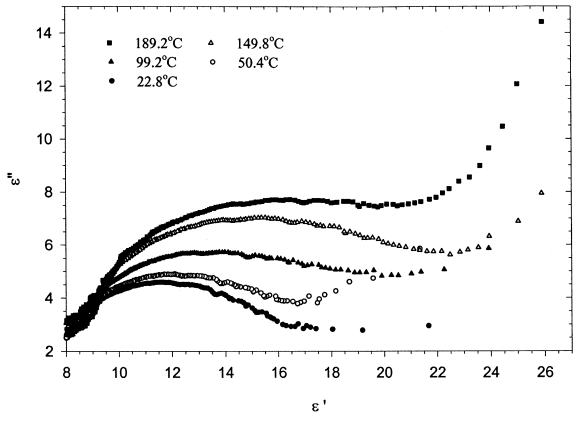

Fig. 7. Cole–Cole plot for Sigma C-3014 kilned peat activated carbon.

Table 1
Summary of Cole–Cole polarization–relaxation parameters

Activated carbon	T (°C)	τ (10^{-11} s)	β	ϵ_{rs} [a]	$\epsilon_{r\infty}$ [b]
Calgon APA	24.0	5.66	0.835	78.0	6.5
Alltech 5769	23.0	6.66	0.770	23.0	6.5
Alltech 5769	50.7	7.04	0.770	24.2	6.5
Alltech 5769	99.2	6.66	0.770	26.9	6.5
Alltech 5769	150.4	5.62	0.820	29.0	6.8
Alltech 5769	188.5	7.04	0.820	31.7	6.8

[a] ϵ_{rs} is the relative static dielectric permittivity (ϵ_s/ϵ_o).
[b] $\epsilon_{r\infty}$ is the relative dielectric permittivity at the high frequency limit ($\varepsilon_\infty/\epsilon_o$).

probably an effect of electrical conductivity of the medium. This type of deviation at low frequencies is far more evident in the Cole–Cole plots for the bituminous activated carbon (Calgon APA) shown in Fig. 6. Here, Eqs. (15) and (16) are applied only to the data acquired at ambient temperature. In marked contrast, the data plotted in Fig. 7. indicates that semicircular symmetry is only vaguely evident in the Cole–Cole plot for the peat bog activated carbon (Sigma C-3014). For this reason, the simple polarization–relaxation model was not applied to this material. The low frequency deviations observed in this material can be explained by an electrical conductivity (σ) term.

$$\varepsilon''(\omega) = \varepsilon_\infty + \frac{\varepsilon_s - \varepsilon_\infty}{1 + i\omega\tau} - \frac{i\sigma}{\omega} \tag{18}$$

Anomalous data in the high frequency regions may originate from the action of two or more independent dielectric relaxors. In the case of two relaxors

$$\varepsilon^*(\omega) = \varepsilon_\infty + \frac{A(\varepsilon_s - \varepsilon_\infty)}{1 + (i\omega\tau_1)^{\beta_1}} + \frac{(1-A)(\varepsilon_s - \varepsilon_\infty)}{1 + (i\omega\tau_2)^{\beta_2}} \tag{19}$$

where A is the fraction of polarizations corresponding to relaxor no. 1 and $1-A$ is the fraction corresponding to relaxor no. 2. This situation can be generalized into systems of n independent relaxors, but analytically it becomes progressively more difficult to derive the corresponding relaxation times and β values.

4. Conclusions

All the activated carbons included in this study absorb microwaves sufficiently to be susceptible to dielectric heating. Considerable variability is evident between the activated carbons, most probably due to the differences in the carbonaceous source material (i.e. peat, coal, and coconut shell) and differences in the activation procedures and post activation treatments. Maxima for the real components of the complex relative permittivities vary between 19 and 110. Maxima for the imaginary components (dielectric loss factors) vary between 4 and 39. The frequencies of maximum dielectric loss range from 1.7 to 4.5 GHz. The dissipation factors at the frequencies of maximum dielectric loss are substantial, ranging between 0.39 and 0.60. Clearly, not all carbons are the same. While it can be said that activated carbons are generally susceptible to dielectric heating via microwave irradiation in the frequency region between 0.9 and 5 GHz (which includes the most common industrial, scientific, and medical microwave frequency bands) it is also evident that, for a given application, the temperature and frequency dependencies of the complex permittivity of the particular material should be considered.

Acknowledgements

This work was funded by the Ames Research Center of the National Aeronautics and Space Administration under contract NAS2-97017. The authors are grateful to Dr. Bernadette K. Luna for her support of this project.

References

[1] Atwater JE, Holtsnider JT, Wheeler Jr. RR. Microwave regenerable air purification device. NASA-CR-201945. Springfield, VA: National Technical Information Service; 1996.
[2] Jackson JD. Classical electrodynamics. New York: Wiley; 1975.
[3] von Hippel A. Dielectrics and waves. New York: Wiley; 1954.
[4] von Hippel A, editor, Dielectric materials and applications, Cambridge: Technology Press of MIT; 1954.
[5] Jonscher AK. Dielectric relaxation in solids. London: Chelsea Dielectrics Press; 1983.
[6] Metaxas AC, Meridith RJ. Industrial microwave heating. London: Peter Perigrinus; 1983.
[7] Atwater JE. Complex permittivities of cyclomaltooligosaccharides (cyclodextrins) over microwave frequencies to 26 GHz. Carbohydr Res 2000;327:219–21.
[8] Atwater JE. Complex dielectric permittivities of the Ag_2O–Ag_2CO_3 system at microwave frequencies and temperatures between 22 and 189°C. Appl Phys A 2002;75:555–8.
[9] Nøst B, Hansen BD, Haslund E. Dielectric dispersion of composite material. Phys Script 1992;T44:67–70.
[10] Polder D, Van Santen JH. The effective permeability of mixtures of solids. Physica 1946;12:257–71.
[11] Stogryn A. The bilocal approximation for the effective dielectric constant of an isotropic random medium. IEEE Trans Antennas Propagat 1984;AP-32:517–20.
[12] Taylor LS. Dielectric properties of mixtures. IEEE Trans Antennas Propagat 1965;AP-13:943–7.
[13] Tsang L, Kong JA. Scattering of electromagnetic waves from random media with strong permittivity fluctuations. Radio Sci 1981;16:303–20.

[14] Sauer RL, Bagdigian RM, editors, Spacecraft water quality: maintenance and monitoring, Warrendale, PA: S.A.E; 1991, pp. 189–94.
[15] Debye P. Polar molecules. Lancaster, PA: Lancaster Press; 1929.
[16] Cole KS, Cole RH. Dispersion and absorption in dielectrics. I. Alternating current characteristics. J Chem Phys 1941;9:341–51.
[17] Davidson DW, Cole RH. Dielectric relaxation in glycerol, propylene glycol, and *n*-propanol. J Chem Phys 1951;19:1484–90.
[18] Ohgushi T, Isimaru K. Dielectric properties of dehydrated NaA zeolite, analyses and calculation of dielectric spectra. Phys Chem Chem Phys 2001;3:3229–34.
[19] Bottcher CJF. Theory of electric polarization. New York: Elsevier; 1952.
[20] Havriliak Jr. S, Havriliak SJ. Dielectric and mechanical relaxation in materials. New York: Hanser; 1997.
[21] Gaiduk VI. Dielectric relaxation and dynamics of polar molecules. New Jersey: World Scientific; 1999.
[22] Jonscher AK. Dielectric relaxation in solids. J Phys D: Appl Phys 1999;32:R57–70.